

Chromatic and spectroscopic signatures of microlensing events as a tool for the gravitational imaging of stars

David Valls–Gabaud^{1,2} *

¹ *URA CNRS 1280, Observatoire de Strasbourg, 11, rue de l'Université, 67000 Strasbourg, France*

² *Royal Greenwich Observatory, Madingley Road, Cambridge CB3 0EZ, UK.*

ABSTRACT

The detection of microlensing events from stars in the Large Magellanic Cloud and in the Galactic bulge raise important constraints on the distribution of dark matter and on galactic structure, although some events may be due to a new type of intrinsic variability. When lenses are relatively close to the sources, we predict that chromatic and spectroscopic effects are likely to appear for a significant fraction of the microlensing events. These effects are due to the differential amplification of the limb and the centre of the stellar disc, and present a systematic dependence with wavelength and time that provide an unambiguous signature of a microlensing event (as opposed to a new type of intrinsic stellar variability). In addition, their measure would provide a direct constraint on stellar atmospheres, allowing a 3-dimensional reconstruction or imaging of its structure, a unique tool to test the current models of stellar atmospheres.

Key words: Cosmology: –gravitational lensing –dark matter, Galaxy: –halo –stellar content, Stars: atmospheres

1 INTRODUCTION

Following the pioneering idea by Paczyński (1986), the detections of several microlensing events from stars in the Large Magellanic Cloud (Alcock *et al.* 1993, 1996; Aubourg *et al.*

* Email: dvg@astro.u-strasbg.fr ; dvg@ast.cam.ac.uk

1993) and of more than 100 from stars in the Galactic bulge (Udalski *et al.* 1993, 1994; Alcock *et al.* 1995, 1997) have raised important constraints on the structure of the different components of our Galaxy. The associated databases containing millions of light curves are also a goldmine for studies in stellar variability (see Ferlet *et al.* 1997, and references therein).

Yet doubts may reasonably be cast on the detections of at least some microlensing events. The two EROS candidates are variable stars : EROS 1 is a Be star (Beaulieu *et al.* 1995), while EROS 2 is an eclipsing binary (Ansari *et al.* 1995). Although spectra of other candidates taken after the event (Della Valle 1994) or during the event itself (Benetti *et al.* 1995; Lennon *et al.* 1996) show no apparent signs of anomalies, the possibility remains that these events are just detections of a new type of variable star. The detection of “bumpers” (Alcock *et al.* 1996), a hitherto unknown type of variable star, and the possibility that dwarf novae and cataclismic variables mimick some events (Della Valle & Livio 1996) are particularly worrying, even though the distribution of the events in the HR diagram indicates that not all the events can be explained by such phenomena. In addition to continuous and follow-up monitoring, it seems important to find unambiguous proofs that the events detected can indeed be associated with microlensing events.

In this context it is interesting to note that the large rate observed towards the bulge may be accounted for if about 50 to 90% of the events are due to lenses within the bulge itself (Kiraga & Paczyński 1994), particularly if the bar is oriented close to the line of sight. The same applies if many of the lenses are within the LMC (Wu 1994; Sahu 1994) or in the halo and bulge of M31.

If this is the case, a significant number of microlensing events should present characteristic chromatic (Valls-Gabaud 1994; Witt 1995; Bogdanov & Cherepaschuk 1995; Gould & Welch 1996) and spectroscopic signatures (Valls-Gabaud 1994; Loeb & Sasselov 1995), and we present in the *Letter* detailed predictions for both effects. These effects arise from the differential amplification between the limb and the inner regions of the stellar disc, where the emerging intensities are different due to the temperature gradient in the atmosphere. The differential amplification also produces a non-zero degree of polarisation during the events (Simmons *et al.* 1995ab), and a spectroscopic line shift (Maoz & Gould 1994).

2 MICROLENSING OF STARS AS EXTENDED SOURCES

The amplification produced by a lens of mass M_L at a distance D_{OL} on a source assumed to be point-like at a distance D_{OS} (Refsdal 1964; Liebes 1964) is $A_p(y) = (y^2 + 2)(y\sqrt{y^2 + 4})^{-1}$ where y is the dimensionless distance between the projected position of the lens and the centre of the source, $y = \sqrt{\alpha_o^2 + (t - t_o)^2/\tau^2}$ and $\alpha_o = \theta_o/\theta_E$, $\tau = D_{OL}\theta_E v_{\perp}^{-1}$ are respectively the minimum dimensionless impact parameter at time t_o , and time scale of the event, with v_{\perp} the transverse velocity of the lens. θ_E is the angular Einstein radius $\theta_E = (4GM_L D_{LS}/c^2 D_{OL} D_{OS})^{1/2}$ where D_{LS} is the distance separating the lens and the source. Since all scales involved are much larger than the wavelength of light, the geometrical optics approximation is valid, and the events should not show diffraction, interference or chromatic effects. Yet, given the colour-magnitude diagrams of the bulge and the LMC, and the sensibility limits of the present surveys, one expects that between one and two thirds of the events are associated with giant stars, so that the point source approximation might be questionable. If the angular radius θ_* of a star of radius R_* seen at a distance D_{OS} is comparable with the angular Einstein radius θ_E of the lens, then effects arising from the finite size of the stars will become apparent. Thus it is only when either the lens mass M_L or the relative distance D_{LS}/D_{OS} is small (or both) that these angles are similar. Although the conditions for this to be true might seem contrived, there will always be a number of microlensing events where the lens will transit through the stellar disc (Gould 1994; Witt 1995). The fraction \mathcal{F} of all lensing events which have a maximum impact parameter smaller than the Einstein radius is simply $\mathcal{F} = \langle \theta_* \rangle \langle 1/\theta_E \rangle$, where average must be taken over the distribution of distances of both lenses and sources, and hence depends on the galactic model adopted. Since the fraction increases like $M_L^{-1/2}$, if the lenses are sub-stellar objects the fraction may reach unity for a large range of D_{LS} distances. However for lenses of $0.1 M_{\odot}$ and typical fractional distances D_{LS}/D_{OS} from 0.1 (bulge) to about $5 \cdot 10^{-3}$ (M31), the fraction of transit events goes from 31% to 16% for typical clump giants of $10 R_{\odot}$. Since they constitute at least a third of the sources, the *minimum* fraction of transit events is around 10% for the bulge and about 5% in M31, for $0.1 M_{\odot}$ lenses. For these events, the sizes of the stars has to be taken into account.

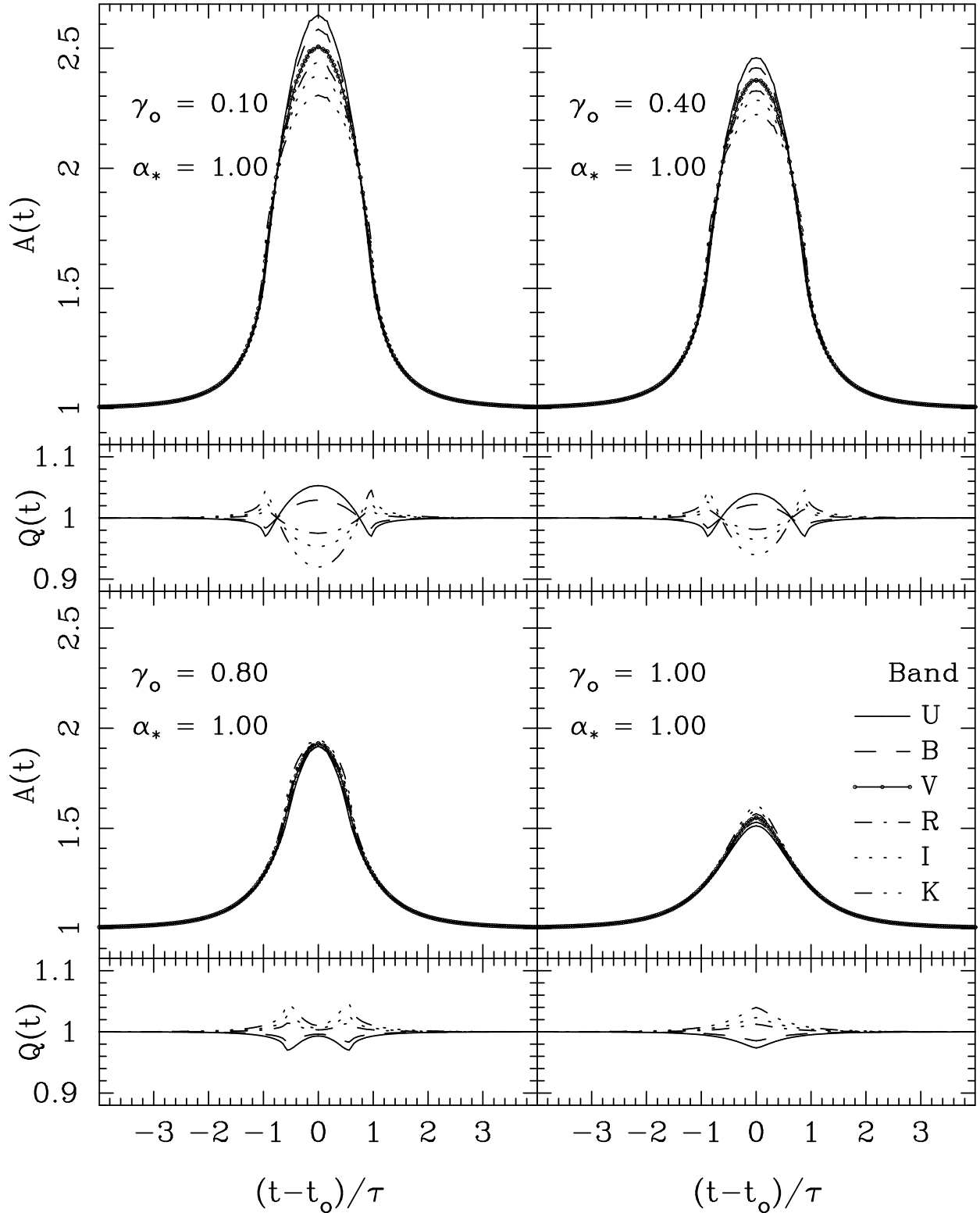


Figure 1. Chromatic signatures of the microlensing of a giant red star of $T_{\text{eff}} = 4000$ K, $\log g = 2.0$ and solar metallicity, for the indicated geometrical parameters [$\gamma_o = \gamma(t_o)$]. The magnifications for the extended Johnson photometric broad bands are calculated assuming a square root non-linear limb darkening profile. The lower panels give the relative magnification relative to the one in the Johnson V band, $Q = A_\lambda/A_V$ which reflects the relative change in colour index $\Delta(m_\lambda - m_V) \approx 1.086(1 - Q)$.

3 CHROMATIC AND SPECTROSCOPIC SIGNATURES

The inclusion of the finite size of the sources was first analysed by Bontz (1979) and more recently by Nemiroff & Wickramasinghe (1994), Gould (1994) and Witt & Mao (1994) for the idealised case of a uniform brightness source, but little attention has been paid so far to the amplification produced by actual stars. Yet it is well known that even in the Eddington approximation the difference in intensity between the centre and the limb of a star reaches almost a magnitude. In the general case then, the magnification A_e of an extended source with specific intensity $\mathcal{I}(\varpi)$ is given by the integration over the extension Ω of the source of the amplification produced on an infinitesimal area on the source at an angular distance θ from the point lens $A_e(\theta) = \int_{\Omega} d\varpi \mathcal{I}(\varpi) A_p(\theta) / \int_{\Omega} d\varpi \mathcal{I}(\varpi)$. Assuming that the star is spherically symmetric (*i.e.*, neglecting rotational flattening, spots, etc.) and using polar coordinates in the source plane and the notation $p^2 = \gamma^2 + x^2 + 2\gamma x \cos \phi$ the actual magnification of the star becomes

$$A_e(\gamma) = \frac{1}{\pi R_{\lambda}} \int_0^{2\pi} d\phi \int_0^1 dx x \mathcal{B}_{\lambda}(x) A_p(p\alpha_*) \quad (1)$$

where $x = r/R_*$, $\alpha_* = \theta_*/\theta_E$, $\gamma = \theta_{\text{LOS}}/\theta_*$ is the angular separation between the lens and the centre of the star in units of the stellar angular radius, $\mathcal{B}_{\lambda}(x) = \mathcal{I}_{\lambda}(x)/\mathcal{I}_{\lambda}(0)$ is the normalised brightness profile, and $R_{\lambda} = 2 \int dx x \mathcal{B}_{\lambda}$ is the dimensionless effective radius at that wavelength. In the case where $\mathcal{B}_{\lambda}(x)$ is constant, the maximum amplification reduces to $A_{\text{uniform}}^{\text{max}} = (1 + 4/\alpha_*^2)^{1/2}$ (Refsdal 1964, Bontz 1979), while for $\gamma \gg 1$, $A_e \rightarrow A_p$, the point-source limit. The brightness profile \mathcal{B}_{λ} is given by the solution of the radiative transfer equation :

$$\mathcal{B}_{\lambda}(x) = \int_0^{\infty} \frac{S_{\lambda}(\tau_{\lambda})}{\mathcal{I}_{\lambda}(0)} \exp \left[-\frac{\tau_{\lambda}}{(1-x^2)^{1/2}} \right] \frac{d\tau_{\lambda}}{(1-x^2)^{1/2}} \quad (2)$$

where $\mathcal{I}_{\lambda}(0)$ is the emerging intensity at the centre of the star and S_{λ} the source function. It is the explicit dependence with wavelength of the brightness profile \mathcal{B}_{λ} and the differential amplification that produce both chromatic and spectroscopic effects (Valls-Gabaud 1994), that reflect the temperature gradient $T(\tau_{\lambda})$ in the stellar atmosphere.

Given a stellar atmosphere model, one derives the corresponding limb profiles for both the continuum and the lines. We have used the large grid of LTE models from Kurucz (1994) and fitted, for the both continuum and a selected set of lines, simple analytical expressions. The reason for this is twofold : first the computational speed is substantially increased, and second the information content of the limb darkening is limited and prevents the use of very detailed

models (Böhm 1961). Since the pioneering studies of Milne (1922), the limb profiles for the continuum are approximated by a linear law $\mathcal{B}_\lambda^{\text{LIN}}(x) = 1 - x_\lambda(1 - \mu)$, where $\mu = (1 - x^2)^{1/2}$. In the modelling of stellar atmospheres, however, non-linear laws have yielded significantly better fits and in particular the logarithmic law $\mathcal{B}_\lambda^{\text{LOG}}(x) = 1 - x_\lambda(1 - \mu) - y_\lambda \mu \ln \mu$ and the square root law (Díaz-Cordovés *et al.* 1995) $\mathcal{B}_\lambda^{\text{SQR}}(x) = 1 - x_\lambda(1 - \mu) - y_\lambda(1 - \sqrt{\mu})$ seem to provide good fits to most of the computed profiles (Van Hamme 1993), although we stress that actual precise data is only available for the Sun. In order to predict the different light curves in the photometric passbands used in microlensing monitoring projects, the limb darkening coefficients are integrated over these bands, and our results agree with those published by Claret & Giménez (1992) and Van Hamme (1993), for both the Johnson and Strömgen systems.

The important point to note is that since the limb darkening coefficients obviously depend on wavelength due to the variation in opacity, different limb profiles will appear depending on the photometric band. This strong dependence with wavelength implies that the same microlensing event will present quite different light curves in different photometric bands, as shown in Fig. 1.

We can understand the behaviour of the light curves as a function of wavelength by noting that the effective radius R_λ increases from 0.64 in the *U* band to 0.90 in the *K* band for the typical red giant star in Fig. 1. Thus, the longer the wavelength, the more uniform the star is, while in the near UV stars are more sharply peaked, giving a larger amplification when the impact parameter is small. At large impact parameters the strong decrease in brightness at shorter wavelengths takes over and the magnification becomes smaller, relative to larger wavelengths. Using the actual limb darkening profiles, the linear Milne law or the non-linear profiles do not make any significant difference ($\Delta A/A \leq 0.01$) in the final magnifications, and hence the use of the linear approximation is fully justified.

One should stress that all these predictions are based on theoretical models which have never been tested in such detail. There may well be further complications, such as for example, at larger wavelengths, in the far IR or sub-mm range, where the limb can actually be brighter (at least in the Sun). In extended envelopes, the increased opacity in the UV can produce a larger R_λ in this domain, and decrease the contrast Q , while in the X-ray domain, the coronal emission is very patchy and a smooth, spherically symmetric distribution is meaningless. There may be also complications related to the presence of chromospheres, which change the temperature gradient and hence the limb profiles. The spectral lines will

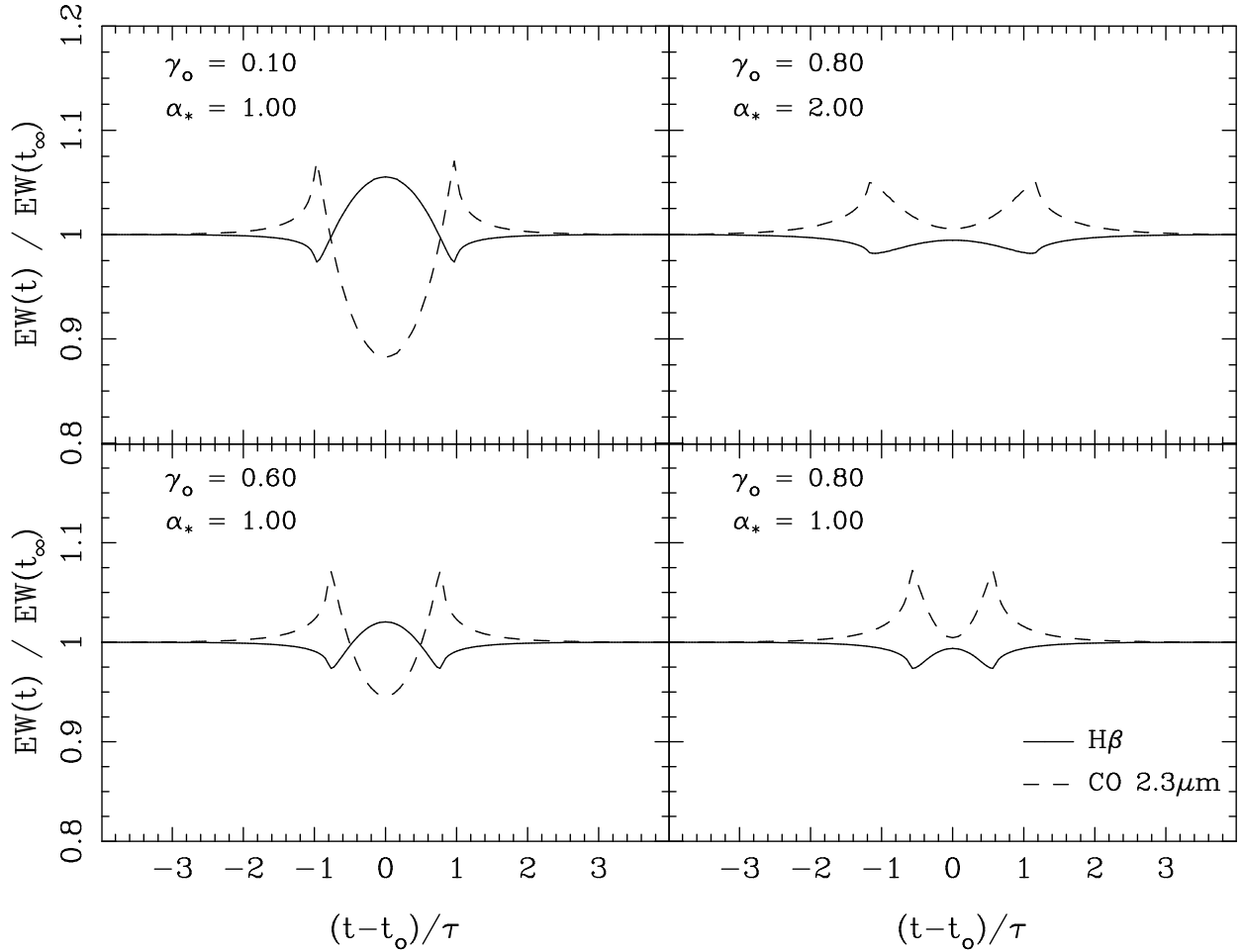


Figure 2. Spectroscopic signatures of microlensing, for the same giant star considered in Fig. 1. and two typical lines : H β and CO 2.3 μm . On the right panels the effect of increasing the stellar diameter (from $\alpha_* = 1$ to $\alpha_* = 2$) is illustrated for the otherwise same transit conditions.

be more sensitive to this effect (see below). To first order, the chromatic effect does not depend on the colour of the stellar source, since the integrated intensity of the star does not appear in Eq. 1. However, there will be some dependence since limb darkening profiles do depend on the spectral type of the star, as well as on the luminosity class. In general, the limb darkening increases when the gravity or temperature decreases and also when the metallicity increases, so the giants of the Galactic and M31 bulges are ideal probes.

The best way to measure the chromatic effect is to observe the event in photometric passbands as widely separated in wavelength as possible, ideally U and K which are the most discriminatory for giant stars. It is unfortunate that the current surveys use bands as close as V , R and I , where the effect is predicted to be very small. As Fig. 1 shows, the relative magnifications Q (with respect to the V band) are smaller than 10%, that is, the change in colour index $\Delta(m_\lambda - m_V) \approx 1.086(1 - Q)$ is less than 0.1 magnitudes, hence it is also essential to do *differential*, rather than absolute, photometry to measure the effect.

Present technology may achieve 0.001 mag (Young *et al.* 1991), although a precision of 0.01 will be enough. Finally, the use of narrow-band Strömgen photometry is also recommended, since the Strömgen bands probe different opacity regimes where the source function changes strongly. The wavelength and time dependence of the light curves are unlike those produced by any intrinsic stellar variability, and hence constitute a unique signature of microlensing events.

The spectroscopic signature arises, once again, because line profiles change significantly across the disc, although in this case the variation will depend on the mechanism of formation of the line. For example strong resonant lines, like Ly- α or Ca II H+K, Mg II $h+k$ present a decreasing relative depression with respect to the continuum, and hence appear brighter at the limb, while pure absorption lines disappear at the limb. Lines are far more sensitive to the actual gradient of temperature in the atmosphere, since they probe a larger range of depths, while others are more sensitive to pressure or turbulence. However, since the observations of the variability of the line profiles seems difficult with the present technology, a more appropriate observable is the equivalent width (EW) of the line. For very strong lines, narrow-band photometry in the appropriate range could also be used (Loeb & Sasselov 1995), but the availability of real-time spectra makes this less practical. To illustrate the predicted behaviour of the EWs during a microlensing event[†], Fig. 2 presents the predictions for the Balmer H β and CO 2.3 μm lines, the CO forming at lower temperature, much higher in the atmosphere, and is limb-brightened. It is immediately apparent that the amplitude of the spectroscopic effect may reach 20%. In the case of H β , which is limb-darkened, the EW first decreases when most of the flux originates from the limb, then increases when the lens is probing the central areas of the star. For the vibrational-rotational bands of CO (from 2.2 to 4.6 μm), the opposite behaviour is present, and the temperature gradient is probed at higher altitude in the atmosphere. Once again, the temporal variation of the lines during the event constitute a unique signature of microlensing, unlike any variation produced by intrinsic stellar variability. Note also that the time scale is no longer the Einstein ring crossing time, but rather the stellar crossing time $\sim R_* v_{\perp} (1 - D_{\text{LS}}/D_{\text{OS}})$ (see Fig. 2).

[†] Detailed predictions for any type of star of metallicity between 0.002 and 0.04 in the wavelength range 1200Å–5 μm are available upon request.

4 DISCUSSION

The gravitational imaging of stars is then possible, where not only the brightness distribution on the stellar disc is measured (via the solution of the integral equation in Eq. 1), but also the source function can be recovered, solving Eq. 2, hence giving a 3-dimensional picture of the stellar atmosphere. This is unprecedented in astrophysics, where only the Sun and very few nearby stars are spatially resolved, either directly (e.g., Gilliland & Dupree 1996) or by interferometry (e.g., Baldwin *et al.* 1996).

Actual techniques for the inversion of Eqs. 1 and 2 cannot fit within the scope of this *Letter*, and will be dealt with elsewhere. We simply note here the important implications of stellar imaging. The predictions presented here are based on model atmospheres, in LTE or NLTE, and the expected limb darkening coefficients have seldom been compared with observations others than the solar ones. The reason is that the only way to measure these coefficients (besides the solar case) accurately is using eclipsing binaries, which must have circular orbits, well-detached components, and produce total eclipses. Even then, the derived coefficients correlate with the assumed sizes of the stars (e.g., Tabachnik 1969), so the measure of limb darkening coefficients in microlensing events is a unique opportunity to test stellar atmosphere models. Note however that the inclusion of non-linear terms produces insignificant differences in the resulting magnification, yet even the measure of the linear coefficients is important, for they provide an estimation of the contribution function of the continuum (basically the integrand of Eq. 2). This in turn gives a direct estimation of the temperature profile, something that is known in very few stars (e.g. Matthews *et al.* 1996) and that provides unprecedented constraints on the opacity sources. This technique, applied to the lines (ideally the profiles, but the EWs are still extremely important) may lead to the element abundance imaging of the star. In general, atmospheric diagnostics will be possible, by selecting lines sensitive to pressure, or temperature, etc.

Unlike Doppler or Zeeman-Doppler imaging, the gravitational imaging is unbiased towards bright stars with large spots, although we note that the presence of spots will considerably complicate the inversion unless the periods are much longer than the time scale of the event. Complications may also arise from blending (Kamionkowsky 1995) and extinction. The ongoing real-time follow-up teams, PLANET (Albrow *et al.* 1997) and GMAN (Abe *et al.* 1997), could adapt their observing strategies to measure these signatures, by increas-

ing the time sampling, widening the wavelength range covered and obtaining the highest resolution spectra possible.

In conclusion, the chromatic and spectroscopic signatures of microlensing events allow us not only to deduce properties of the lenses, but also, and maybe more importantly, to open an entire new window on stellar atmospheres.

ACKNOWLEDGEMENTS

I am grateful to W. Van Hamme and A. Claret for providing their latest limb darkening calculations for comparison with ours.

Note: After this paper was completed, Alcock *et al.* (1997, ApJ, submitted, astro-ph 9702199) have reported real-time photometry and spectroscopy of events associated with a M4 giant in the Galactic bulge. Both signatures may be present, although further analysis is required for confirmation.

REFERENCES

- Abe, F. *et al.* (GMAN coll.) 1997 in *Variable stars and astrophysical returns of microlensing surveys*, R. Ferlet *et al.* (eds), Ed. Frontières, in press
- Albrow, M. *et al.* (PLANET coll.) 1997 in *Variable stars and astrophysical returns of microlensing surveys*, R. Ferlet *et al.* (eds), Ed. Frontières, in press
- Alcock, C. *et al.* (MACHO coll.) 1993, *Nature* **365**, 621
- Alcock, C. *et al.* (MACHO coll.) 1995, *ApJ* **445**, 133
- Alcock, C. *et al.* (MACHO coll.) 1996, *ApJ* **461**, 84
- Alcock, C. *et al.* (MACHO coll.) 1997, *ApJ* **479**, 119
- Ansari, R. *et al.* (EROS coll.) 1995, *A&A* **299**, L21
- Aubourg, E. *et al.* (EROS coll.) 1993, *Nature* **365**, 623
- Baldwin, J.E. *et al.* 1996, *A&A* **306**, L13
- Beaulieu, J.P. *et al.* (EROS coll.) 1995, *A&A* **299**, 168
- Benetti, S. Pasquini, L. & West, R.M. 1995, *A&A* **294**, L37
- Bogdanov, M.B. & Cherepashchuk, A.M. 1995, *Astr. Rep.* **39** 873
- Böhm, K.-H. 1961, *ApJ* **134**, 264
- Bontz, R.J. 1979, *ApJ* **233**, 402
- Claret, A. & Giménez, A. 1990, *A&A* **230**, 412
- Della Valle, M. 1994, *A&A* **287**, L31
- Della Valle, M. & Livio, 1996, *ApJ* **457**, L77
- Díaz-Cordovés, J., Claret, A. & Giménez, A. 1995, *A&A Suppl.* **110**, 329
- Ferlet, R., Maillard, J.P. & Raban, B. 1997, *Variable stars and astrophysical returns of microlensing surveys*, Editions Frontières, in press
- Gilliland, R.L. & Dupree, A.K. 1996, *ApJ* **463**, L29
- Gould, A. 1994, *ApJ* **421**, L71
- Gould, A. & Welch, D.L. 1996, *ApJ* **464**, 212

- Kiraga , M. & Paczyński, B. 1994, ApJ **430**, L101
- Kurucz, R.L. 1994, Atlas CDROMs
- Kamionkowski, M. 1995, ApJ **442**, L9
- Liebes, S. 1964, Phys. Rev. **133**, 835
- Lennon, D.J., Mao, S., Fuhrmann, K. & Gehren, T. 1996, ApJ **471**, L23
- Loeb, A. & Sasselov, D. 1995, ApJ **449**, L33
- Maoz, D. & Gould, A. 1994, ApJ **425**, L67
- Matthews, J.M., Wehlau, W.H., Rice, J. & Walker, G.A.H. 1996, ApJ **459**, 278
- Milne, E.A., 1922, Phil. Trans. Roy. Soc., **A223**, 201
- Nemiroff, R.J. & Wickramasinghe, W. 1994, ApJ **424**, L21
- Paczynski, B. 1986, ApJ **304**, 1
- Refsdal, S. 1964, MNRAS **128**, 295
- Sahu, K.C. 1994, Nature **370**, 275
- Simmons, J.F.L., Willis, J.P. & Newsam, A.M. 1995a, A&A **293**, L46
- Simmons, J.F.L., Newsam, A.M. & Willis, J.P. 1995b, MNRAS **276**, 182
- Tabachnik, V.M. 1968, Astron. Zh. **45**, 1048
- Udalski, A., *et al.* (OGLE coll.) 1993, Acta Astron. **43**, 289.
- Udalski, A., *et al.* (OGLE coll.) 1994, Acta Astron. **44**, 1.
- Valls-Gabaud, D. 1994, in *Large scale structures in the universe*, J. Mücke *et al.* (eds), World Scientific, p. 326
- Van Hamme, W. 1993, AJ **106**, 2096
- Witt, H.A. 1995, ApJ **449**, 42
- Witt, H.A. & Mao, S. 1994, ApJ **430**, 505
- Wu, X.-P. 1994, MNRAS **435**, 66
- Young, A.T., *et al.* 1991, PASP **103**, 221